SUPPLEMENTARY MATERIAL FOR

Myxobacterial depsipeptide chondramides interrupt SARS-CoV-2 entry by targeting its broad, cell tropic spike protein

Rey Arturo Fernandez[a], Mark Tristan Quimque[a,b,c], Kin Israel Notarte[d], Joe Anthony H. Manzano[a,e], Delfin Yñigo Pilapil IV[a,e], Von Novi de Leon[a,e], John Jeric San Jose[a], Omar Villalobos[f], Nisha Harur Muralidharan[g], M. Michael Gromiha[g], Simone Brogi[h], Allan Patrick G. Macabeo[a],*

[a]Laboratory for Organic Reactivity, Discovery and Synthesis (LORDS), Research Center for the Natural and Applied Sciences, University of Santo Tomas, España Blvd., Manila1015, Philippines

[b]The Graduate School, University of Santo Tomas, España Blvd., Manila 1015, Philippines

[c]Chemistry Department, College of Science and Mathematics, Mindanao State University – Iligan Institute of Technology, Tibanga, 9200 Iligan City, Philippines

[d]Faculty of Medicine and Surgery, University of Santo Tomas, España Blvd., Manila 1015, Philippines

[e]Department of Biological Sciences, College of Science, University of Santo Tomas, España Blvd., Manila 1015, Philippines

[f]Department of Pharmacy, Faculty of Pharmacy, University of Santo Tomas, España Blvd., Manila 1015, Philippines

[g]Department of Biotechnology, Bhupat and Jyoti Mehta School of Biosciences, Indian Institute of Technology (IIT) Madras, Chennai 600 036, Tamilnadu, India

[h]Department of Pharmacy, University of Pisa, Via Bonanno 6, 56126, Pisa, Italy

*Corresponding author: agmacabeo@ust.edu.ph / allanpatrick_m@yahoo.com; Tel No. +632-34061611 local 4057; Fax No. +632-87314-031.

Table of Contents

	Page
Figure S1. Chemical structures of the myxobacterial secondary metabolites **1-24**.	4
Figure S2. Chemical structures of the myxobacterial secondary metabolites **24-48**.	5
Figure S3. Chemical structures of the myxobacterial secondary metabolites **49-72**.	6
Figure S4. (A) Superposition between the docking output from AutoDock Vina (grey surface for the protein and green sticks for the ligand) and Glide considering the Brazilian variant (pink sticks for the ligand), RMSD of 1.011 Å; (B) superposition between the docking output from AutoDock Vina (grey surface for the protein and green sticks for the ligand) and Glide considering the South African variant (cyan sticks for the ligand), RMSD of 0.717 Å; (C) superposition between the docking output from AutoDock Vina (grey surface for the protein and green sticks for the ligand) and Glide considering the UK variant (yellow sticks for the ligand), RMSD of 0.936 Å; (D) superposition between the docking output from AutoDock Vina (grey surface for the protein and green sticks for the ligand) and Glide considering the wild type protein (magenta sticks for the ligand), RMSD of 0.984 Å.	7
Table S1. Docking scores of myxobacterial secondary metabolites **1-72** against SARS-CoV-2 spike protein receptor-binding regions.	8
Table S2. Summary of the binding energies (BE) and interacting residues of the top compounds against SARS-CoV-2 spike wild-type and variants I472V, A475V and L452Y.	10
Table S3. Summary of the binding energies (BE) and interacting residues of the top compounds against SARS-CoV-2 spike wild-type and variants V438A, F490L, S477N and N439K	11
Table S4. List of active residues set and protein-protein dock poses during protein-protein docking of spike against host receptors.	12
Table S5. Summary of binding energies of top compounds against spike RBD for ACE2 or GRP78, ACE2, and GRP78 based on selectivity docking.	13
Table S6. Lipinski's Rule of Five for ADME analysis of compounds **1–8**.	13

Table S7. Predicted toxicity parameters and solubility of compounds **1–8**. 14

Table S8. Docking grid coordinates of SARS-CoV-2 spike proteins and host receptors. 14

References 14

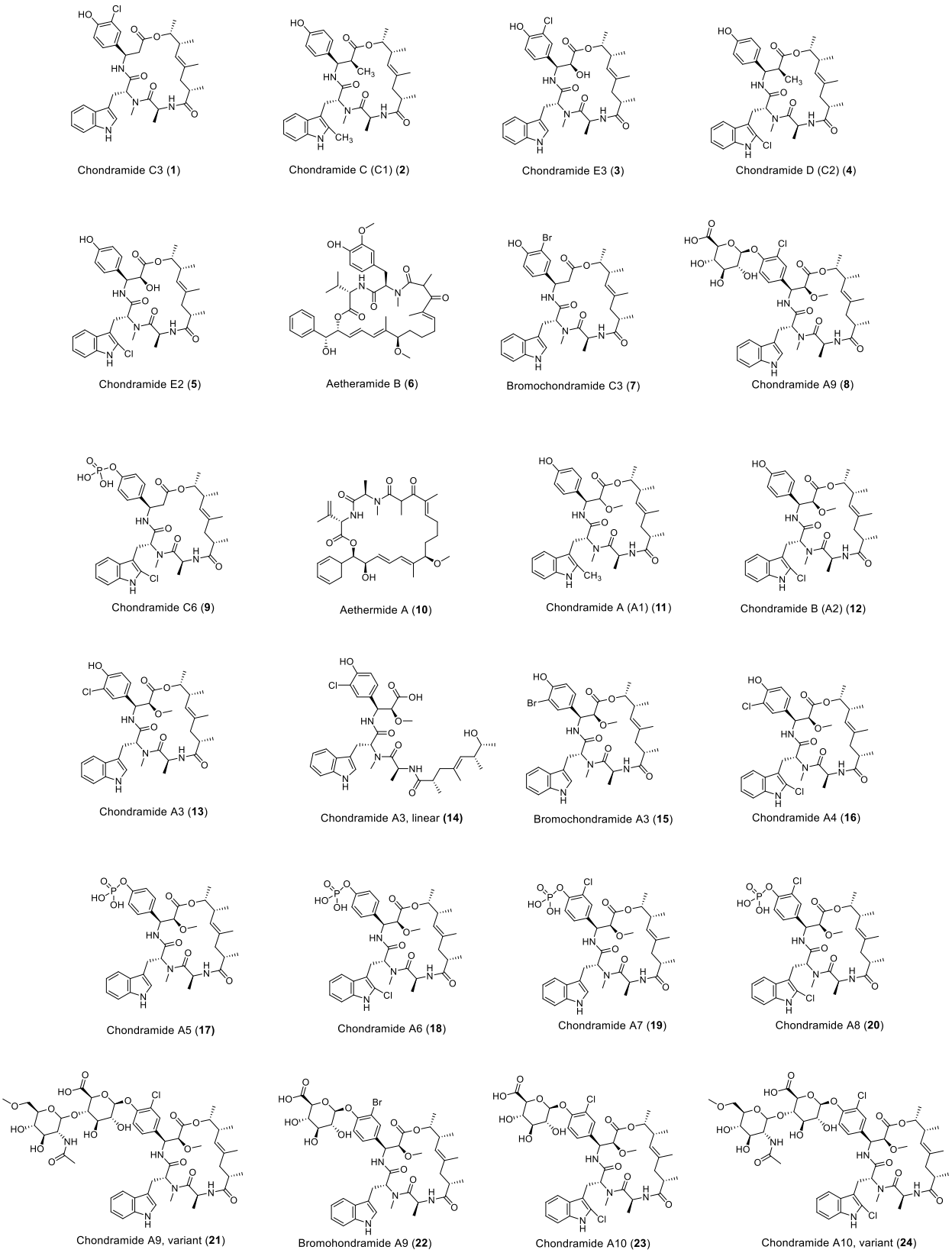

Figure S1. Chemical structures of the myxobacterial secondary metabolites **1-24.**

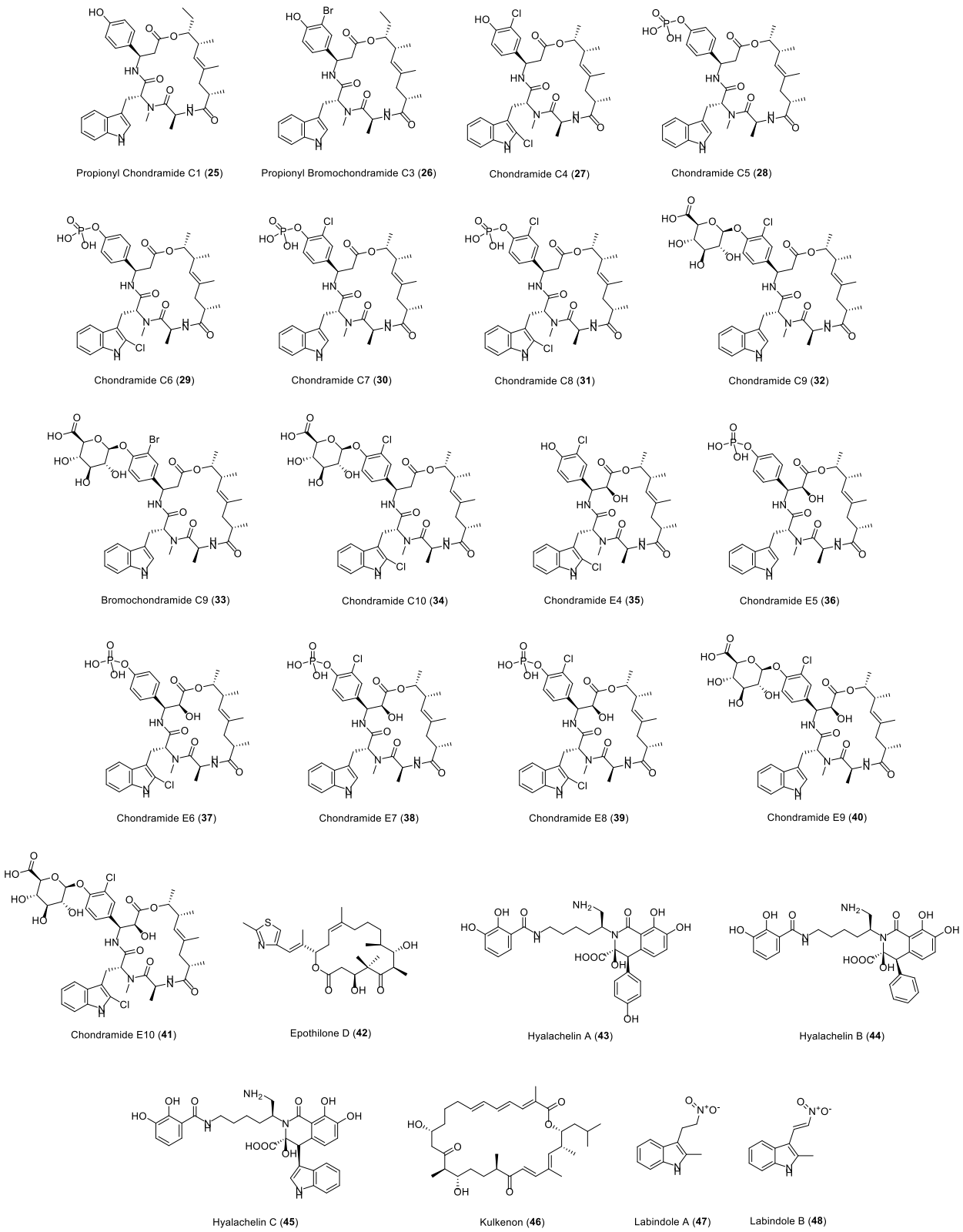

Figure S2. Chemical structures of the myxobacterial secondary metabolites **25-48**.

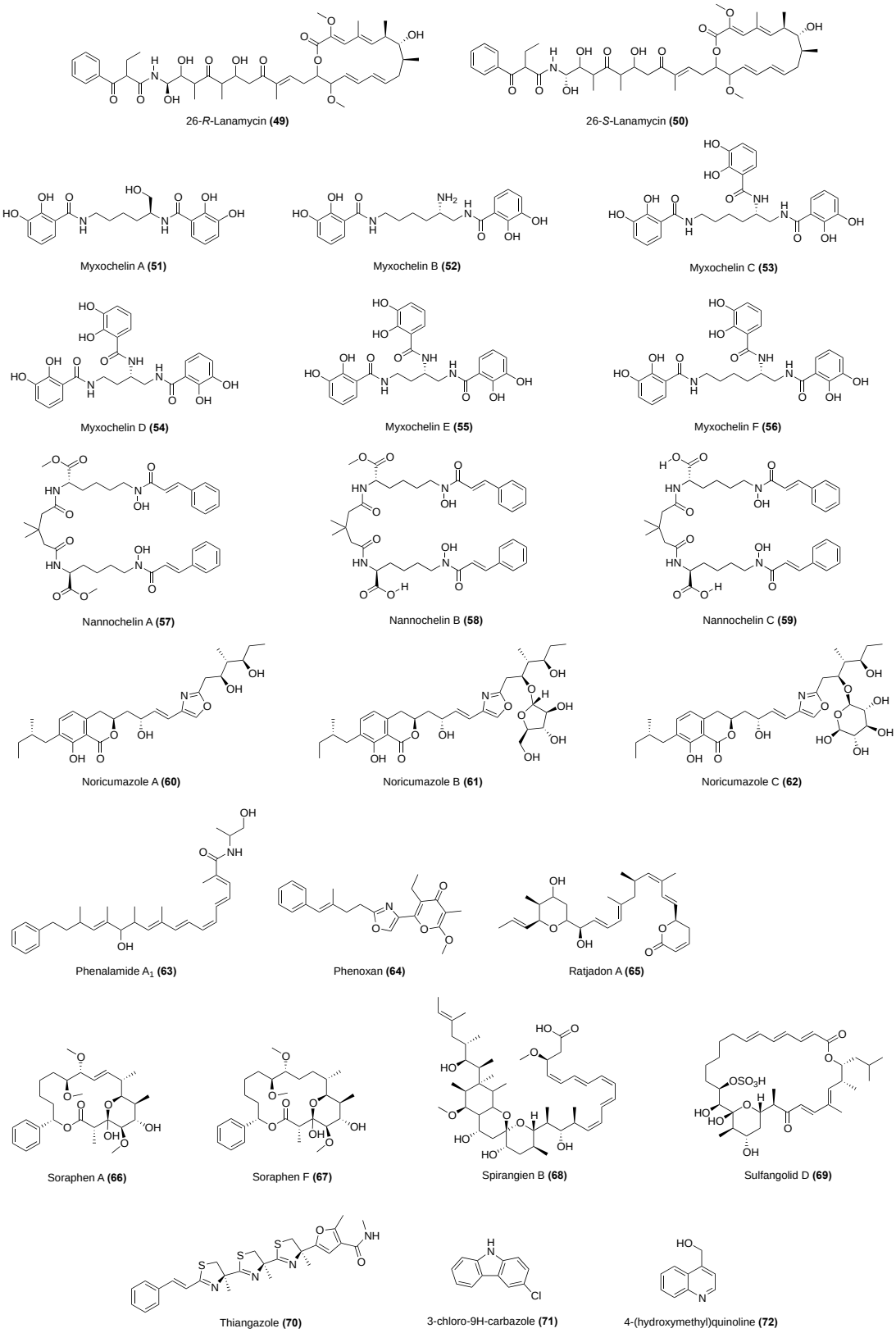

Figure S3. Chemical structures of the myxobacterial secondary metabolites **49-72**.

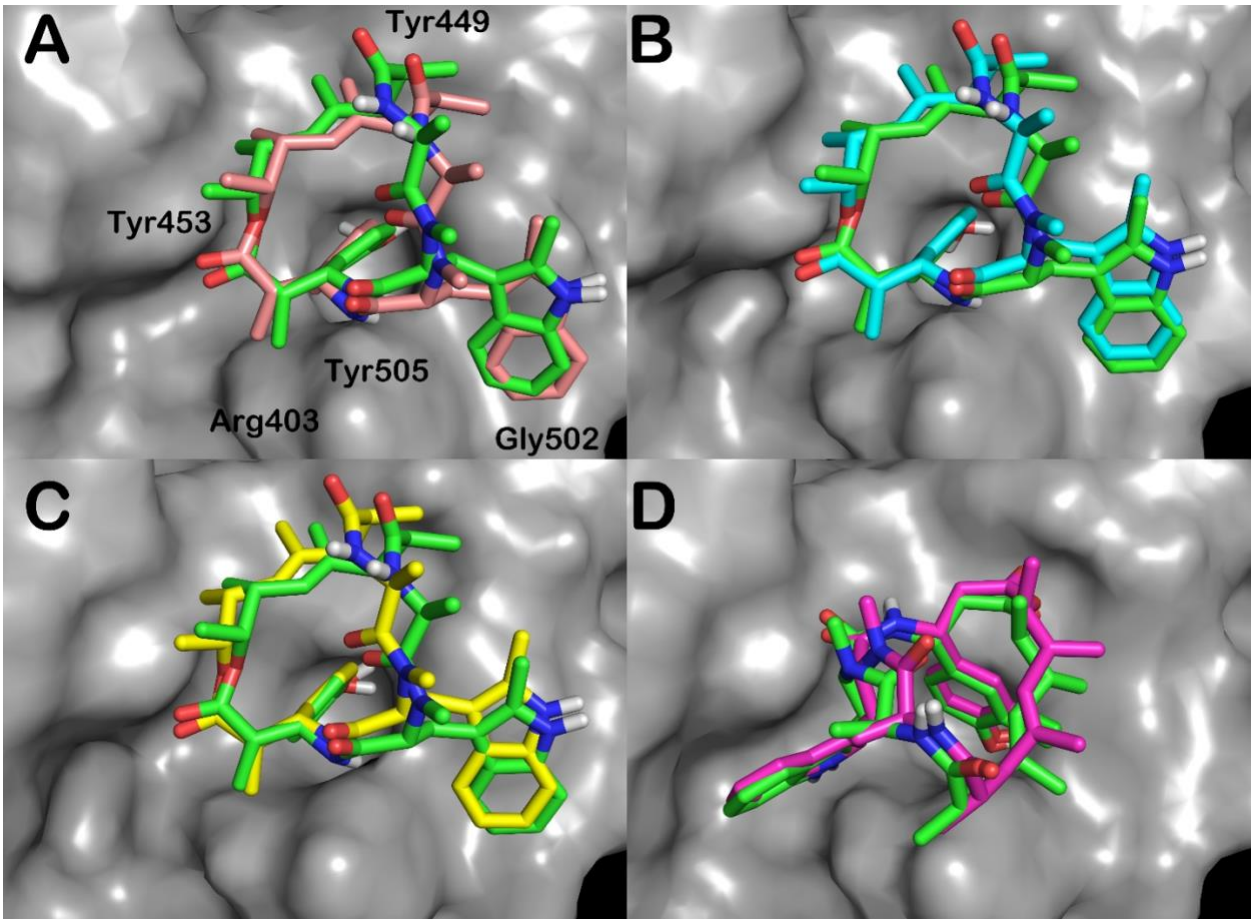

Figure S4. (A) Superposition between the docking output from AutoDock Vina (grey surface for the protein and green sticks for the ligand) and Glide considering the Brazilian variant (pink sticks for the ligand), RMSD of 1.011 Å; (B) superposition between the docking output from AutoDock Vina (grey surface for the protein and green sticks for the ligand) and Glide considering the South African variant (cyan sticks for the ligand), RMSD of 0.717 Å; (C) superposition between the docking output from AutoDock Vina (grey surface for the protein and green sticks for the ligand) and Glide considering the UK variant (yellow sticks for the ligand), RMSD of 0.936 Å; (D) superposition between the docking output from AutoDock Vina (grey surface for the protein and green sticks for the ligand) and Glide considering the wild type protein (magenta sticks for the ligand), RMSD of 0.984 Å.

Table S1. Docking scores of myxobacterial secondary metabolites **1-72** against SARS-CoV-2 spike protein receptor-binding regions.

Cpd	Binding energy (kcal/mol)			Cpd	Binding energy (kcal/mol)		
	ACE2 RBD	GRP78 RBD	NRP1 binding region		ACE2 RBD	GRP78 RBD	NRP1 binding region
1	-8.7	-7.6	-4.3	**22**	-7.7	-7.7	-5.6
2	-8.6	-7.9	-5.2	**23**	-7.3	-8.3	-4.9
3	-8.4	-7.6	-6.1	**24**	-7.1	-8.5	-5.3
4	-8.4	-7.8	-4.9	**25**	-7.4	-8.2	-5.3
5	-8.2	-8.3	-4.8	**26**	-7.6	-7.3	-4.4
6	-8.1	-7.7	-6.3	**27**	-7.7	-8.3	-6.1
7	-8.1	-7.8	-5.7	**28**	-7.1	-7.7	-4.7
8	-8	-8.7	-5.2	**29**	-7.6	-8.8	-5.1
9	-7.2	-7.4	-4.0	**30**	-7.5	-8.0	-4.8
10	-7.4	-7.4	-5.2	**31**	-7.0	-7.6	-4.8
11	-7.9	-7.7	-5.1	**32**	-7.7	-8.2	-5.7
12	-7.5	-7.9	-5.3	**33**	-7.1	-8.1	-6.0
13	-6.2	-7.3	-5.1	**34**	-7.2	-7.6	-5.9
14	-7.7	-7.7	-4.3	**35**	-7.9	-7.8	-5.1
15	-7.5	-7.3	-5.9	**36**	-7.0	-8.0	-4.9
16	-7.5	-7.5	-5.4	**37**	-7.7	-7.6	-5 .2
17	-7.5	-7.6	-5.7	**38**	-6.8	-7.3	-5.0
18	-7.5	-7.4	-5.6	**39**	-7.4	-7.3	-4.5
19	-7.3	-8.5	-5.4	**40**	-7.6	-8.4	-5.2
20	-7.8	-7.8	-5.4	**41**	-7.4	-7.3	-5.6
21	-7.4	-8.0	-5.5	**42**	-6.5	-7.2	-5.1

Cpd	Binding energy (kcal/mol)			Cpd	Binding energy (kcal/mol)		
	ACE2 RBD	GRP78 RBD	NRP1 binding region		ACE2 RBD	GRP78 RBD	NRP1 binding region
43	-6.8	-7.7	-4.9	**58**	-6.3	-7.6	-5.2
44	-6.8	-7.6	-5.9	**59**	-6.6	-7.1	-4.6
45	-6.6	-6.9	-5.7	**60**	-6.3	-7.6	-6.0
46	-6.8	-7.1	-5.1	**61**	-6.4	-7.2	-4.9
47	-6.5	-5.6	-4.9	**62**	-6.6	-7.2	-6.0
48	-6.3	-5.7	-5.2	**63**	-5.1	-6.3	-4.2
49	-7.4	-7.8	-5.1	**64**	-6.5	-7.4	-5.8
50	-6.7	-7.6	-5.4	**65**	-6.3	-7.3	-4.8
51	-6.7	-6.9	-5.0	**66**	-6.0	-5.7	-4.0
52	-6.2	-7.3	-5.8	**67**	-5.6	-5.8	-4.4
53	-6.9	-6.8	-5.3	**68**	-5.9	-6.7	-4.3
54	-6.6	-7.5	-5.8	**69**	-6.5	-6.6	-5.4
55	-6.4	-7.7	-5.4	**70**	-7.4	-8.4	-6.5
56	-5.8	-7.6	-5.1	**71**	-6.0	-6.0	-5.7
57	-6.1	-5.8	-4.6	**72**	-5.3	-5.4	-4.9

Table S2. Summary of the binding energies (BE) and interacting residues of the top compounds against SARS-CoV-2 spike wild-type and variants I472V, A475V and L452Y.

Compounds	I472V			A475V			L452R		
	BE	**Conventional H-bonding**	**Other types of molecular interactions**	**BE**	**Conventional H-bonding**	**Other types of molecular interactions**	**BE**	**Conventional H-bonding**	**Other types of molecular interactions**
Chondramide C3 (1)	**-8.7**	Glu406, Tyr449, Tyr453, Ser494, Tyr495, Tyr505	Arg403 (π-cation), Lys417 (π-alkyl), Tyr453 (π-π stacked), Tyr505 (π-alkyl)	**-8.4**	Glu406, Tyr453, Ser494, Gly496	Arg403 (π-cation), Gly496 (π-donor hydrogen bond) Tyr505 (π-alkyl), Gly496 (C-H bond)	**-8.5**	Glu406, Tyr453, Ser494, Asn501,	Arg403 (π-cation), Tyr453 (π-π stacked), Gly496 (π-donor hydrogen bond), Tyr505 (π-alkyl) Gly496 (C-H bond)
Chondramide C (2)	**-8.6**	Tyr453, Asn501, Tyr505	Tyr449 (π-alkyl), Tyr505 (π-alkyl, π-π stacked and π-π *T*-shaped)	**-8.3**	Tyr449	Arg403 (π-cation), Tyr453 (π-π stacked), Gly496 (π-donor hydrogen bond), Tyr505 (π-alkyl)	**-8.3**	Tyr449, Tyr505	Arg403 (π-cation), Tyr453 (π-π stacked), Gly496 (π-donor hydrogen bond), Tyr505 (π-alkyl)
Chondramide E3 (3)	**-8.4**	Glu406, Tyr453, Tyr449, Ser494, Asn505	Arg403 (π-cation), Tyr453 (π-π stacked), Gly496 (π-donor hydrogen bond)	**-7.3**	Gly496, Asn501	Arg403 (π-cation), Tyr505 (π-π stacked)	**-8.2**	Gly496, Gln498	Arg403 (π-cation), Tyr453 (π-π stacked), Tyr505 (π-alkyl, π-π stacked and π-π *T*-shaped)
Chondramide D (4)	**-8.3**	Tyr453, Gly496	Tyr449 (π-alkyl), Tyr505 (π-π stacked and π-π *T*-shaped)	**-8.2**	Tyr453, Asn501, Tyr505	Tyr449 (π-alkyl), Tyr505 (π-π stacked and π-π *T*-shaped)	**-8.2**	Tyr453, Gly496, Tyr505	Tyr449 (π-alkyl), Tyr505 (π-π stacked and π-π T-shaped)
Chondramide E2 (5)	**-8.2**	Tyr449, Gln498, Asn501	Tyr449 (π-alkyl), Tyr505 (π-π stacked)	**-7.9**	Gly496, Asn501	Arg403 (π-cation), Tyr449 (π-π stacked), Tyr505 (π-π T-shaped)	**-7.9**	Gly496, Asn501	Arg403 (π-cation), Tyr453 (π-π stacked), Tyr505 (π-π stacked and π-π *T*-shaped)
Aetheramide B (6)	**-8**	Arg403, Asn501	Lys417 (π-alkyl), Tyr489 (π-π T-shaped), Gly496 (π-donor hydrogen bond), Tyr505 (π-π T-shaped and alkyl)	**-8.1**	Arg403, Gly496, Asn501	Gly496 (π-donor hydrogen bond) Asn501 (C-H bond)	**-8.1**	Arg403, Asn501, Tyr505	Tyr489 (π-π T-shaped), Gly496 (π-donor hydrogen bond)
Bromo-chondramide C3 (7)	**-8**	Tyr453, Asn501, Tyr505	Tyr505 (π-π stacked and π-π T-shaped)	**-6.6**	Ser494, Gly496, Gln498	Tyr495 (π-alkyl), Tyr505 (π-π T-shaped) Gly496 (C-H bond)	**-8**	Glu406, Tyr453, Ser494, Gly496, Tyr505	Arg403 (π-cation), Lys417 (π-alkyl), Tyr453 (π-π stacked), Gly496 (π-donor hydrogen bond)
Chondramide A9 (8)	**-8.7**	Glu406, Tyr449, Tyr453, Ser494, Tyr495, Tyr505	Arg403 (π-cation), Lys417 (π-alkyl), Tyr453 (π-π stacked), Tyr505 (π-alkyl)	**-7.7**	Ser349, Asn450, Gln493	Tyr449 and Leu452 (π-alkyl), Phe490 (π-π stacked)	**-8.3**	Thr470, Gly482, Leu492, Gln493, Ser494	Phe490 (π-π stacked), Gly482 (C-H bond)

Table S3. Summary of the binding energies (BE) and interacting residues of the top compounds against SARS-CoV-2 spike wild-type and variants V438A, F490L, S477N and N439K.

Cpd	V483A			F490L			S477N			N439K		
	BE	**Conventional H-bonding**	**Other types of molecular interactions**	**BE**	**Conventional H-bonding**	**Other types of molecular interactions**	**BE**	**Conventional H-bonding**	**Other types of molecular interactions**	**BE**	**Conventional H-bonding**	**Other types of molecular interactions**
1	**-8.5**	Glu406, Tyr453, Ser494, Asn501	Arg403 (π-cation), Tyr453 (π-π stacked), Gly496 (π-donor hydrogen bond), Tyr505 (π-alkyl), Gly496 (C-H bond)	**-8.5**	Glu406, Tyr453, Ser494, Asn501	Arg403 (π-cation), Tyr453 (π-π stacked), Gly496 (π-donor hydrogen bond), Tyr505 (π-alkyl), Gly496 (C-H bond)	**-8.5**	Glu406, Tyr453, Ser494, Gly496, Tyr505	Arg403 (π-cation), Lys417 (π-aklyl), Tyr453 (π-π stacked), Gly496 (π-donor hydrogen bond), Tyr505 (π-alkyl), Gly496 (C-H bond)	**-8.4**	Glu406, Tyr453, Ser494, Asn501	Arg403 (π-cation), Tyr453 (π-π stacked), Gly496 (π-donor hydrogen bond), Tyr505 (π-alkyl) Gly496 (C-H bond)
2	**-8.4**	Tyr453, Asn501, Tyr505	Tyr449 (π-alkyl), Tyr505 (π-π T-shaped and π-alkyl)	**-8.3**	Tyr449	Arg403 (π-cation), Tyr453 (π-π stacked), Gly496 (π-donor hydrogen bond), Tyr505 (π-alkyl)	**-8.4**	Tyr453, Gly496, Asn501	Tyr449 (π-alkyl), Tyr505 (π-π T-shaped and π-alkyl)	**-8.3**	Tyr449, Tyr505	Arg403 (π-cation), Tyr453 (π-π stacked), Gly496 (π-donor hydrogen bond), Tyr505 (π-alkyl) Gly496 (C-H bond)
3	**-8.2**	Gly496	Arg403 (π-cation), Tyr453 (π-π stacked), Tyr505 (π-π stacked and π-alkyl)	**-7.4**	Gly496, Gln498	Arg403 (π-cation), Tyr453 (π-π stacked), Tyr505 (π-π stacked and π-π T-shaped)	**-7.4**	Gly496	Arg403 (π-cation), Tyr505 (π-π stacked)	**-7.4**	Gly496, Gln498	Arg403 (π-cation), Tyr505 (π-π stacked)
4	**-8.3**	Tyr453, Asn501, Tyr505	Tyr449 (π-alkyl), Tyr505 (π-π stacked and π-π T-shaped)	**-8.2**	Tyr453, Gly496, Tyr505	Tyr449 (π-alkyl), Tyr505 (π-π stacked and π-π T-shaped)	**-8.2**	Arg403, Asn501, Tyr505	Tyr449 (π-alkyl), Tyr505 (π-π stacked and π-π T-shaped)	**-8.2**	Arg403, Asn501, Tyr505	Tyr449 (π-alkyl), Tyr505 (π-π stacked and π-π T-shaped)
5	**-7.9**	Gly496, Asn501	Arg403 (π-cation), Tyr453 (π-π stacked), Tyr505 (π-π stacked and π-π T-shaped)	**-7.9**	Gly496, Gln498	Arg403 (π-cation), Tyr453 (π-π stacked), Tyr505 (π-π stacked and π-π T-shaped)	**-7.9**	Gly496	Arg403 (π-cation), Tyr453 (π-π stacked), Tyr505 (π-π stacked and π-π T-shaped)	**-7.9**	Gly496	Arg403 (π-cation), Tyr453 (π-π stacked), Tyr505 (π-π stacked and π-π T-shaped)
6	**-8.1**	Arg403, Asn501	Tyr489 (π-π T-shaped), Gly496 (π-donor hydrogen bond), Tyr505 (π-alkyl), Gly496 (C-H bond)	**-8**	Arg403, Asn501, Tyr505	Tyr489 (π-π T-shaped), Gly496 (π-donor hydrogen bond), Gly496 and Asn501 (C-H bond)	**-8.1**	Arg403, Gly496, Asn501	Arg403 (π-cation), Lys417 (Alkyl), Tyr489 (π-alkyl) Gly496 and Asn501 (C-H bond)	**-8.1**	Arg403, Gly496	Lys417 (π-alkyl), Tyr489 (π-π T-shaped) Gly496 (C-H bond)
7	**-7.8**	Ser494, Gly496, Gln498	Tyr505 (π-π T-shaped and π-alkyl), Gly496 (C-H bond)	**-6.6**	Ser494, Gly496, Gln498	Tyr505 (π-alkyl and π-π T-shaped), Gly496 (C-H bond)	**-7.8**	Tyr453, Asn501, Tyr505	Tyr505 (π-π stacked and π-π T-shaped)	**-6.6**	Ser494, Gly496, Gln498	Tyr505 (π-π T-shaped and π-alkyl) Gly496 (C-H bond)
8	**-8.2**	Asn450, Gln493	Tyr449 and Leu452 (π-alkyl), Tyr449 (C-H bond)	**-7.6**	Tyr449, Gln493, Ser494	Tyr505 (π-alkyl), Tyr495 and Gly496 (C-H bond)	**-7.7**	Ser494, Gln498	Tyr505 (π-alkyl) and Gly496 (C-H bond)	**-7.7**	Phe347, Ser349, Asn450, Gln493	Tyr449 and Leu452 (π-alkyl)

Table S4. List of active residues set and protein-protein dock poses during protein-protein docking of spike against host receptors.

Receptor	Active Residues		Dock poses
	Spike protein	Host receptor	
ACE2	403-505	24-393	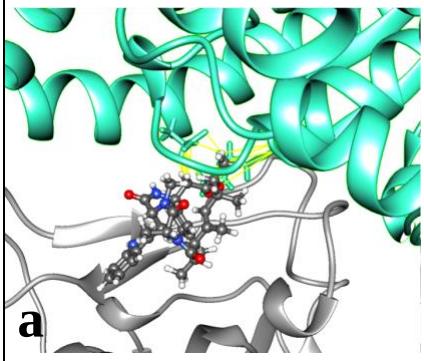
GRP78	479-481	428-458	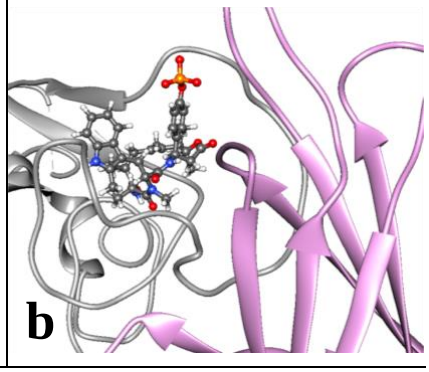

Protein-protein docking poses showing ligand-protein atomic clash of (a) spike RDB/chondramide C3 - ACE2 complex and (b) spike RBD/chondramide C6 – GRP78 complex.

Table S5. Summary of binding energies of top compounds against spike RBD for ACE2 or GRP78, ACE2, and GRP78 based on selectivity docking.

Cpd	Binding Energy (kcal/mol)					
	Spike RBD				ACE2	GRP78
	Wild type	N501Y	E484K	D614G		
1	-8.7	-	-	-	-6.1	-
2	-8.6	-9.1	-8.7	-8.3	-7.0	-
9	-8.8	-	-	-	-	-6.6

These compounds emerged as top chondramides against spike RBDs for ACE2 (Cpd 1 and 2) and GRP78 (Cpd 9). In addition, Cpd 2 is summarized with BEs against the variants due to high affinities despite mutations (see Table 1).

Table S6. Lipinski's Rule of Five for ADME analysis of compounds **1–9.**

Cpd	MW (<500)	#H-bond acceptors (<10)	#H-bond donors (<5)	MLOGP (<5)	Lipinski #violations	Drug Likeness
1	651.19	6	4	2.45	1	YES
2	616.75	6	4	2	1	YES
3	667.19	7	5	1.68	2	NO
4	651.19	6	4	2.45	1	YES
5	667.19	7	5	1.68	2	NO
6	718.88	9	3	1.88	1	YES
7	695.64	6	4	2.53	1	YES
8	857.34	13	7	-0.41	3	NO
9	731.17	9	5	1.74	2	NO

Table S7. Predicted toxicity parameters and solubility of compounds **1–9**.

Cpd	Toxicity Risks			
	Mutagenicity	Tumorigenicity	Irritant effect	Reproductive toxicity
1	None	None	None	None
2	None	None	None	None
3	None	None	None	None
4	None	None	None	None
5	None	None	None	None
6	None	None	Medium-risk	None
7	None	None	None	None
8	None	None	None	None
9	None	None	None	None

Table S8. Docking grid coordinates of SARS-CoV-2 spike proteins and host receptors.

Protein (PDB ID)	Coordinates			Protein (PDB ID)	Coordinates		
	x	y	z		x	y	z
SARS-CoV-2 RBD to ACE2 (6M0J)	-38	30	5	ACE2 (6M0J, chain A)	-30	30	0
SARS-CoV-2 RBD to GRP78 (6VXX)	210	178	262	GRP78 (5E84)	23	60	-33

REFERENCES:

(1) Herrmann, J.; Hüttel, S.; Müller, R. Discovery and biological activity of new chondramides from *Chondromyces* sp. *Chembiochem*, **2013**, *14* (13), 1573–1580. https://doi.org/10.1002/cbic.20130 0140.

(2) Mulwa, L. S., & Stadler, M. (2018). Antiviral compounds from Myxobacteria. Microorganisms, 6(3), 73–88. https://doi.org/10.3390/microorganisms6030073.